Separation Science and Technology
Publication details, including instructions for authors and subscription information:
http://www.informaworld.com/smpp/title~content=t713708471

Effect of H^+ and N^+ Irradiation on Structure and Permeability of the Polyimide Matrimid®

Ling Hu[a]; Xinglong Xu[a]; Maria R. Coleman[a]
[a] Department of Chemical & Environmental Engineering, University of Toledo, OH, USA

To cite this Article Hu, Ling , Xu, Xinglong and Coleman, Maria R.(2008) 'Effect of H^+ and N^+ Irradiation on Structure and Permeability of the Polyimide Matrimid®', Separation Science and Technology, 43: 16, 4030 — 4055
To link to this Article: DOI: 10.1080/01496390802414734
URL: http://dx.doi.org/10.1080/01496390802414734

Separation Science and Technology, 43: 4030–4055, 2008

ISSN: 0149-6395 print/1520-5754 online
DOI: 10.1080/01496390802414734

Taylor & Francis
Taylor & Francis Group

Effect of H^+ and N^+ Irradiation on Structure and Permeability of the Polyimide Matrimid®

Ling Hu, Xinglong Xu, and Maria R. Coleman
Department of Chemical & Environmental Engineering,
University of Toledo, OH, USA

Abstract: This paper presents a comparison of the impact of H^+ and N^+ ion irradiation on the chemical structure, microstructure, and gas permeation properites of the polyimide, Matrimid®. While irradiation with both ions resulted in evolution of chemical structure with loss of functional groups and crosslink formation, there was greater modification of polyimide structure following N^+ irradiation at similar total deposited energy. Irradiation with N^+ resulted in simultaneous large increases in permeance and permselectivity at comparatively low ion fluences or irradiation time. For example, irradiation at 4×10^{14} N^+/cm^2 resulted in a 2.5 fold increase in He permeance with a selectivity of He/CH_4 of 340. Much higher H^+ fluences were required to achieve similar total deposited energy and combined increases in permeance and permselectivity. The larger modification in chemical structure and gas permeation properties following N^+ irradiation was attributed to the relatively large energy loss and damage from the nuclear energy relative to electronic energy loss.

Keywords: Crosslinking, ion beam irradiation, gas separation membrane, hydrogen, permeability, polyimide

INTRODUCTION

Membrane based gas separation systems have found increasing commercial application because of there flexible design, lower energy

Received 7 December 2007; accepted 2 July 2008.
Address correspondence to Maria R. Coleman, Department of Chemical & Environmental Engineering, University of Toledo, 2801 West Bancroft St., Toledo, OH 43606, USA. Tel.: 1 (419) 530 8091; Fax: 1 (419) 530 8086. E-mail: maria.coleman6@utoledo.edu

expenditure, and ease of operation in comparison with conventional methods (1–7). Numerous studies have reported development of polymeric membrane materials that have attractive gas separation properties (i.e., high gas permeability and high permselectivity) combined with thermal and mechanical stability (1–3). These studies mainly focus on

(i) synthesis of polymers designed using structure-property relationship (1–7), and
(ii) development of alternative membrane materials and/or modification of existing polymeric membranes using diverse post-synthesis techniques (8–26).

Targeted polymer synthesis based on developing materials with combined high free volume and chain rigidity has led to classes of polymers with attractive transport properties (1–7). However, synthesis of new materials is costly and it is increasingly difficult to synthesize processible polymers with significantly improved gas transport properties. Post-synthesis methods that modify the structure and microstructure of existing polymeric membranes to optimize the gas transport properties are attractive alternatives to new polymer synthesis. These methods include thermal treatment (4–7), fluorination (8–10), plasma treatment (11–15), and ion beam irradiation (15–25). Ion beam irradiation allows selective modification of the chemical structure, microstructure and properties of polymers. In addition, the thin surface selective layer of asymmetric membranes can be modified without affecting the porous support through careful selection of irradiation conditions (25). With careful selection of irradiation conditions, on beam irradiation has the potential to modify both permeability and permselectivity of industrial interesting gas pairs.

Two earlier papers by our group focused on a detailed study of the impact of H^+ irradiation on chemical structure and pure gas permeation properties of the polyimide, Matrimid® (16,17). Matrimid® has superior gas transport properties to many commercial polymers for industrially important gas pairs (H_2/CH_4, O_2/N_2, and CO_2/CH_4,) and has well characterized physical and transport properties (3). Therefore, Matrimid® was an ideal system for studying the impact of ion irradiation on gas transport properties. H^+ irradiation resulted in degradation of the polymer backbone structure with loss of functional groups and formation of crosslinks at higher fluences, as well as increases in permeance of small gas molecules with smalls increases in permselectivity. While the irradiation results for permeation properties were promising, the extent of modification by H^+ irradiation was limited by range of fluence that were possible in a reasonable time frame and lower relative damage from small

atom. This paper presents a comparison of the impact of $H+$ and N^+ irradiation at similar total deposited energies on the structural evolution and gas permeation properties of the polyimide, Matrimid®. N^+ has the potential for greater damage to polymer backbone structure for similar irradiation conditions.

BACKGROUND

The impact of ion beam irradiation on the structure and properties of polymers is a strong function of the ion type, ion energy and the fluence, and the structure of the base polymer (26–38). During irradiation, energetic ions undergo a series of collisions with atoms and electrons in the near surface region of the sample where the incident ion loses energy through interactions with the polymer. Energy transfer from incident ions to a polymer can result in a number of chemical reactions within the polymer through including degradation of chemical bonds with formation of free radicals, release of small volatile molecules, and crosslink formation between polymer chains. The evolution in chemical structure will result in a corresponding modification in the polymer microstructure through a combination of formation of crosslinks and small molecular size defects resulting from release of small molecules. This would result in a shift in the overall polymer fractional free volume, free volume distribution as well as chain mobility, thus modifying gas transport properties of the polymeric membrane (17–23). For example, positron annihilation spectroscopy of N^+ irradiated polyimide indicated that there was both an increase in free volume and the generation of a new population of defects (i.e. free volume packets) that correlated well with modification in gas permeation properties (21).

There are two energy loss or transfer mechanisms from incident ions to polymers in the energy range used in this study:

(i) Electronic energy or inelastic energy loss involves electronic excitation and ionization of target atoms and exchange of electrons between incident ion and polymer. Electronic collision involves much smaller energy loss per collision, negligible deflection of the ion trajectory, and negligible lattice disorder (26).
(ii) Nuclear energy or elastic energy loss primarily involves atomic collision between ion and atoms in the polymer. Nuclear collisions involve a considerable discrete energy loss and angular deflection of the trajectory of the ion, which is responsible for direct bond breaking and production of lattice disorder by the displacement of atoms. Each of these mechanisms contributes quite differently to modification of chemical structure, and microstructure of polymers (35).

While both electronic and nuclear energy loss mechanisms are important in determining the final structure and properties of irradiated polymers, nuclear energy loss tends to result in greater damage to the polymer structure in irradiated layer and evolution in properties at similar total deposited energy relative to electron energy loss (26,29–37). Irradiating ions with higher atomic number exhibit larger relative nuclear contribution and generally result in greater evolution in properties at similar total deposited energy.

The relative contributions to the total energy deposition from the nuclear and electronic loss mechanisms can be determined using a well establish Monte Carlo simulation method (SRIM code) (39). An example of depth profiles of the energy loss mechanisms for 450 keV H^+ and 3400 keV N^+ ions in the polyimide, Matrimid®, used for this study is illustrated in Fig. 1. For H^+ irradiation, the electronic energy loss dominated with negligible nuclear energy loss. However, for N^+ irradiation, there was a measurable nuclear energy loss that is much smaller than the electronic energy loss over a whole penetration depth. For H^+ ion beam irradiation the electronic energy, loss is relatively flat over a large portion

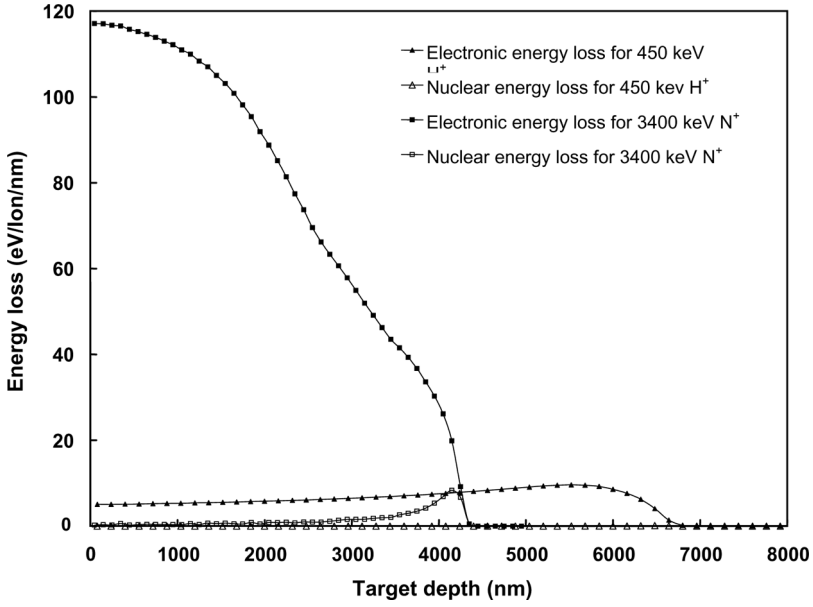

Figure 1. Depth profiles of energy loss mechanisms of ions in the Matrimid® thin films used for structural evolution studies at 450 keV for H^+ irradiation and 3400 keV for N^+ irradiation. The depth profile was estimated using the SRIM monte carlo simulation (39).

of the depth range, whereas for N^+ irradiation the electronic energy loss decreases with the penetration depth. The mean projected range (R_p) of ion into the polymer surface increased with ion energy and decreased with increasing atomic number of the ion. Therefore, irradiation conditions can be readily adjusted to control the depth of modification.

The impact of irradiation on a polymer can be compared in terms of ion fluence or dosage with units of ions/irradiated surface area or total deposited energy with units of eV/irradiated volume. The total deposited energy is the product of the total energy stopping power of ion dE/dx (i.e. the average deposited energy) and ion fluence (26,39). The total electronic energy loss and the total nuclear energy loss are defined with respect to the electronic stopping power of ion (i.e. the average electronic energy loss) and the nuclear stopping power of ion (i.e. the average nuclear energy loss) times ion fluence. For each irradiated sample, the average nuclear energy loss, the average electronic energy loss and the average deposited energy were estimated by applying Equation (1) to SRIM energy deposition profiles for N^+ and H^+ irradiation of Matrimid®:

$$\left(\frac{dE}{dx}\right)_i = \frac{\int_0^l (dE/dx)_{i,x} dx}{l} \quad (1)$$

where $(dE/dx)_i$ is the average electronic (or nuclear) energy loss or the average deposited energy, $(dE/dx)_{i,x}$ is the electronic (or nuclear) energy loss or the deposited energy at depth of x calculated using SRIM code, x penetrating depth of ion, and l the thickness of the sample. The total deposited energy increases with ion energy and the atomic number of the ion so that lower ion doses or fluences are required to achieve similar total deposited energies within the irradiated region (26,39). The ion fluences used for H^+ and N^+ irradiation in this study were designed so that the total deposited energies for both cases would fall in the same range. Much lower fluences were required for N^+ irradiation to reach similar total deposited energies, which can significantly reduce the required irradiation time. According to Equation 1 and the depth profiles shown in Fig. 1, the nuclear energy loss for N^+ and H^+ used for this study were approximately 2–7% and 0.1%, respectively, of the total deposited energy.

Although the electronic energy transfer increased proportionally with the total deposited energy for both ions, there was no significant deviation in the total electronic energy loss between N^+ and H^+ over this range. There was an increase in relative contribution to total deposited energy from the nuclear energy loss for N^+ irradiation with a much smaller increase for H^+ irradiation. Therefore, increasing the total

deposited energy through increasing ion fluence tended to result in larger differences in the total nuclear energy loss between N^+ and H^+ irradiation. At lower fluences N^+ and H^+ irradiation where electronic energy loss mechanism dominates for both ions were expected to have similar effect structure of the Matrimid®. However, as fluences (and total deposited energy) were increased the nuclear energy loss was more important in determining the polymer modification for the larger irradiating ion. Since there is greater modification to polymer structure and microstructure following irradiation with ions that exhibit greater nuclear energy loss, N^+ irradiation will tend to result in greater evolution in structure and properties of the Matrimid® than H^+ irradiation (26,29–37).

EXPERIMENTAL

Materials and Membrane Formation

Matrimid® was purchased in powder form from Ciba Specialty Chemicals Company (New Jersey) and methylene chloride (CH_2Cl_2) from Fisher Scientific. All of the chemicals were reagent grade and used without further purification. Free-standing thin films produced using a method described in detail elsewhere were used for FTIR and dissolution studies (16). For this method, a solution of $5 \sim 7$ wt% Matrimid® in methylene chloride was poured on a 4" polished silicon wafer on a spin coater (P-6000 Spin Coater from Specialty Coating System, Inc.) and spun at $400 \sim 700$ rpm for about 6 minutes. The film was masked with aluminum foil, removed from the wafer, and dried in a vacuum oven at 80°C to remove residual solvent. All film thicknesses measured using a digital micrometer were approximately 6.5 μm for H^+ irradiation and 3.8 μm for N^+ irradiation.

Permeances of the virgin and irradiated membranes were determined using composite membranes that consisted of a very thin Matrimid® selective layer on a porous ceramic membrane (17). Whatman® anodisc membranes with pores of 0.02 μm pore diameter provided an inert mechanical support to isolate the impact of ion beam irradiation on Matrimid® bulk transport properties. A solution of 3–6 wt% Matrimid® in methylene chloride was prepared and cast on an anodisc membrane using a spin-coating method (17). The O_2/N_2 ideal selectivity of each virgin Matrimid®-ceramic composite membrane was greater than 75% of the reported bulk material value ($\alpha_{O_2/N_2} = 6.11$ (3) and $\alpha_{O_2/N_2} = 6.8$ (38)). The polymer selective layer of the unmodified composite membranes was relatively defect-free. Based on the O_2 permeability of the bulk material and O_2 permeances of the virgin membranes, the approximate

average thickness of selective layers of the membranes used for H^+ and N^+ irradiation was between 0.3 and 1.3 μm.

Ion Beam Irradiation

Ion beam irradiation was performed at room temperature within a vacuum chamber at a pressure less than 1.9×10^{-7} torr of a Tandem Accelerator at the University of Western Ontario, London, Ontario, Canada. To avoid overheating of the sample, low beam-current density ($<1\ \mu A/cm^2$) was used with the incident beam perpendicular to the surface of the samples. As discussed earlier and outlined in detail elsewhere, the required incident energy of irradiation was determined using a well-known program titled "The Stopping and Range of Ion in Matter" (SRIM) to ensure that the whole thickness of the film was modified (39). For FTIR analysis, 450 keV H^+ and 3400 keV N^+ ions were chosen based on the measured thickness of the Matrimid® free-standing films used. For gas permeation study, 180 kev H^+ and 400 keV N^+ ions were chosen based on the estimated selective layer thickness of the Matrimid-ceramic composite membranes. The calculated percentage of the nuclear energy loss in the total deposited energy for 3400 keV N^+ and 450 keV H^+ irradiation of FTIR samples were approximate 2% and 0.1%, respectively. The calculated percentage of the nuclear energy loss of the total deposited energy for the composite membrane 400 keV N^+ and 180 keV H^+ irradiation of permeation samples were approximately 5–7% and 0.1%, respectively. The fluence ranges used for this study (7×10^{12} to $3 \times 10^{15}\ H^+/cm^2$ and 6×10^{11} to $1.5 \times 10^{15}\ N^+/cm^2$) were selected to allow irradiation over similar total deposited energies for both ions. Note that much lower fluences are required to achieve similar total deposited energy for N^+ irradiation. A summary of the calculated projected ranges and irradiation conditions is given in Table 1.

Table 1. Calculated projected ranges of H^+ and N^+ ions at different energies calculated using SRIM to allow modification of entire membrane thickness

Sample type (thickness)	Ion energy/Type	Projected range R_p (μm)
Structural evolution (6.5 μm)	450 keV H^+	7.0
Structural evolution (3.8 μm)	3400 keV N^+	4.5
Composite membrane (0.3–1.3 μm)	180 keV H^+	2.4
Composite membrane (0.6–0.9 μm)	400 keV N^+	1.2

Characterization of Structural Evolution

Fourier Transform Infrared Spectroscopy (FTIR) was used to study the evolution of Matrimid® structure following ion beam irradiation. All measurements were performed using a Nicolet FT-IR 5DV spectrometer at the Instrumention Center of the University of Toledo. The same analysis conditions were used before and after ion beam irradiation for each sample to monitor any change of the spectrum induced by irradiation. A detailed analysis of the relative peak area for functional groups was used to monitor the impact of irradiation conditions on evolution of polymer properties (16).

The dense films used for FTIR study were used for dissolution studies in methylene chloride to probe the onset of irradiation-induced crosslinking. A small piece of each sample was immersed in an excess volume of methylene chloride in a small sealed tube at room temperature. Methylene chloride is a commonly used solvent for polyimides and easily dissolves Matrimid® within minutes. The tubes were stored at room temperature for several hours and in a refrigerator at $4 \sim 6°C$ to minimize evaporation losses of solvent and observed after one month. Any dissolution of irradiated samples occurred within a few hours at room temperature so no change was observed during storage.

Gas Permeation Measurements

The pure gas permeances were measured in following order for the virgin and the irradiated membranes of He, O_2, N_2, CO_2, and CH_4 in a standard constant volume variable pressure permeation cell at 35°C with pressurized upstream and evacuated downstream (17). The standard method used for characterizing polymer membranes was modified to prevent stress on the ceramic porous support. For these experiments, the upstream side of the membrane was purged at low pressure with the feed gas instead of evacuating prior to a run. After purging the feed for several minutes, the downstream was slowly evacuated, the upstream purge was closed and the feed pressure increased to 55 psig overnight prior to permeation measurements. The permeance is the pressure normalized flux of a gas through a membrane and is a function of the membrane permeability and thickness of selective layer. The selective layer thickness was estimated using the reported O_2 permeability of the bulk material and O_2 permeance of the virgin membrane (3). Relative permeances and permselectivities will be used to compare the impact of ion type, total deposited energy, and ion fluence on transport properties of the different membranes to eliminate the effects of film thickness on the resulting properties.

The relative permeance is the ratio of the permeance of the membrane following irradiation to the permeance of virgin membrane.

RESULTS AND DISCUSSION

Evolution in Matrimid® Backbone Structure

The evolution in chemical structure of the Matrimid® following ion beam irradiation was was monitored using both FTIR analysis and dissolution studies (16). Partial dissolution or insolubility in methylene chloride provided a qualitative measure of onset of crosslinking following ion irradiation. The dissolution results in terms of ion fluence and total deposited energy for both the 450 keV H^+ and 3400 keV N^+ irradiated Matrimid® films are summarized in Table 2. While irradiation with both ions eventually resulted in crosslinking, much lower ion fluences and total deposited energies were required for onset of crosslinking following N^+ irradiation than H^+. For example, N^+ irradiated Matrimid® films were partially soluble at $5.8 \times 10^{11}\,N^+/cm^2$ and totally insoluble at $4.2 \times 10^{12}\,N^+/cm^2$. A much higher fluence and total deposited energy was required to induce crosslinking following H^+ irradiation. Crosslinking studies suggested that N^+ irradiation induced much larger modification to chemical structure of the polyimide Matrimid® than did H^+ irradiation.

Table 2. Impact of ion fluence on dissolution of the irradiated Matrimid® films in excess methylene chloride at room temperature

	Ion fluence (Ion/cm^2) or Total deposited energy (eV/cm^3)	
Dissolution results	450 keV H^+ ion irradiation	3400 keV N^+ ion irradiation
Completely dissolved	7×10^{12} to $1 \times 10^{13}\,H^+/cm^2$ 4.8×10^{18} to $6.8 \times 10^{18}\,eV/cm^3$	None
Partially dissolved	5×10^{13} to $3 \times 10^{14}\,H^+/cm^2$	5.8×10^{11} to $8.3 \times 10^{11}\,N^+/cm^2$
	3.4×10^{19} to $2.1 \times 10^{20}\,eV/cm^3$	5.1×10^{18} to $7.2 \times 10^{18}\,eV/cm^3$
No noticeable dissolution	6×10^{14} to 3×10^{15}	4.2×10^{12} to $8.3 \times 10^{13}\,N^+/cm^2$
	4.0×10^{20} to $2.1 \times 10^{21}\,eV/cm^3$	3.6×10^{19} to $7.2 \times 10^{20}\,eV/cm^3$

A spectrum of the virgin Matrimid® and samples of spectrum following irradiation in the range of 400 to 4000 cm^{-1} are shown in Fig. 2 (a) and (b). The FTIR spectra of all the virgin films were consistent with the Matrimid® spectra reported in the literature (16). Four bands, located at 1778, 1725, 1374, and 1096 cm^{-1}, respectively, are characteristic of

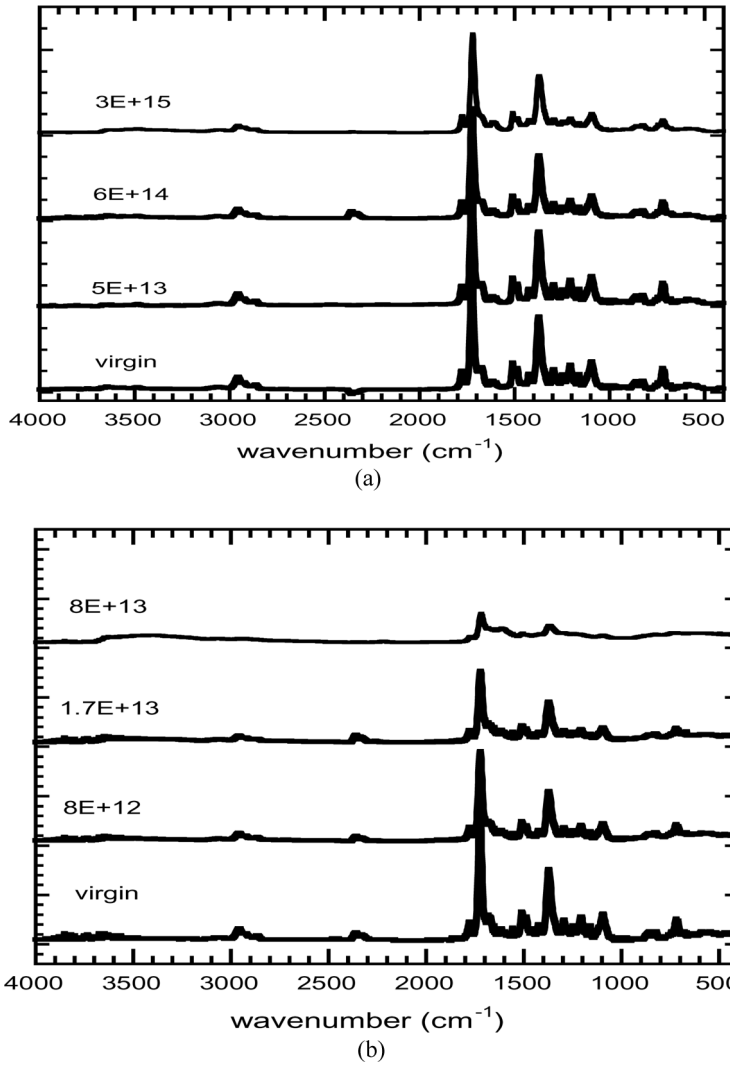

Figure 2. FTIR spectra for Matrimid® films irradiated with both 450 keV H^+ ion (a) and 3400 keV N^+ ion (b) at different ion fluences.

the imide groups of Matrimid®. The infrared band assignments and structure of the Matrimid® are listed in Table 3 to facilitate reading of the FTIR spectrum. There was a general trend of loss of peaks for several functional groups along the backbone with increasing ion fluence for both irradiating ions indicate degradation of the backbone structure.

The normalized areas of three functional bands of the Matrimid® (i.e. the aliphatic stretching mode, the imide I C=O stretching mode and the aromatic stretching mode of the para-disubstituted phenyl) are plotted as a function of ion fluence in Fig. 3 (a) and total deposited energy in Fig. 3 (b). The normalized area is the ratio of the area of the band of the Matrimid® following ion beam irradiation (A) to the area of the band of the virgin Matrimid® (A_0). The structural evolution of the Matrimid® following H^+ irradiation was discussed in detail elsewhere so only a brief review is included (16). Specifically, the aliphatic methyl (CH_3) bond and the benzophenone C=O were more sensitive to H^+ irradiation than groups along the backbone including the imide groups and the para-disubstituted aromatic ring. At low ion fluences (below $5 \times 10^{13}\,H^+/cm^2$), the films were completely soluble and H^+ irradiation resulted in no noticeable crosslinking. For $5 \times 10^{13}\,H^+/cm^2$, there was partial crosslinking, which was attributed to degradation of the aliphatic

Table 3. Structure and characteristic absorbance bands for the polymer Matrimid® in the range of 400–4600 cm^{-1}

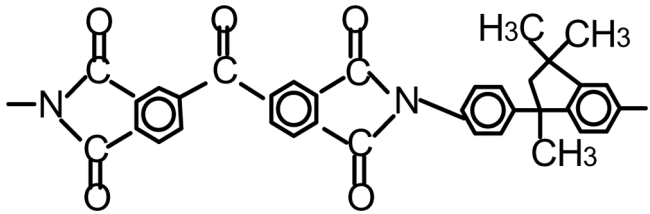

Number	ν (cm^{-1})	Band assignment
1a	2960–2860	CH stretching of methyl
1b	3062	Aromatic CH stretching
2a	1778	Symmetric C=O stretching (imideI)
2b	1725	Asymmetric C=O stretching (imideI)
3	1676	C=O stretching of benzophenone carbonyl
4&4′	1512&1488	C=C stretching of para-disubstituted aromatic ring
5	1374	CNC axial stretching (imideII)
6	1096	CNC transverse stretching (imideIII)
7	3450–3500	OH stretching

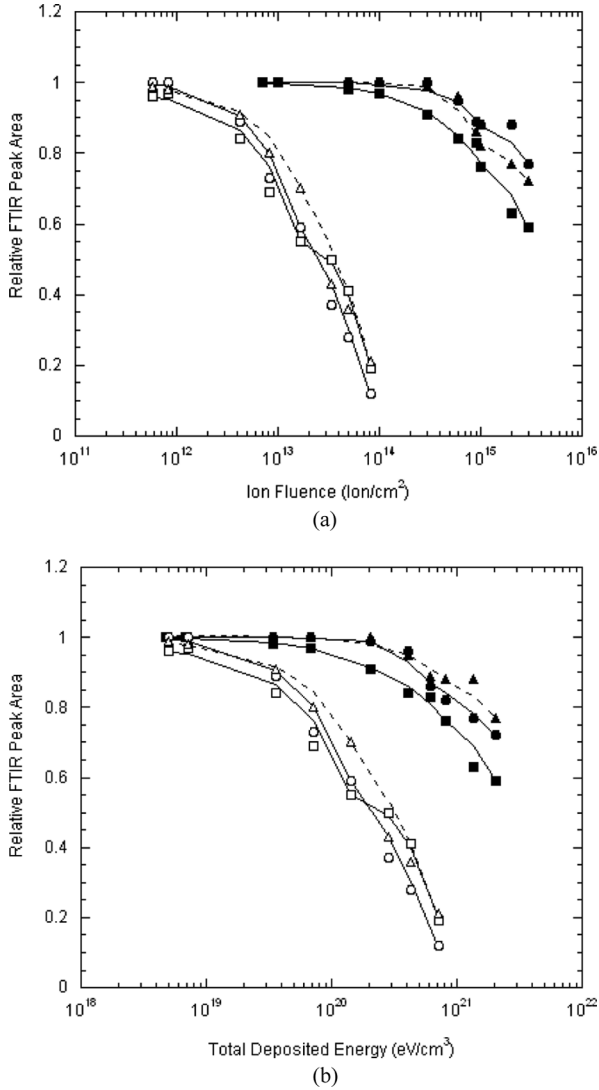

Figure 3. (a) Normalized areas of the characteristic absorption bands attributed to the aliphatic stretch group (□,■), the imide I C=O (△,▲), and the para-disubstituted aromatic ring (○,●) versus ion fluence for Matrimid® irradiated with 450 keV H^+ ion represented by closed symbols or 3400 keV N^+ ions represented by open symbols. (b) Normalized areas of the characteristic absorption bands attributed to the aliphatic stretch group (□,■), the imide I C=O (△,▲), and the para-disubstituted aromatic ring (○,●) versus the total deposited energy for Matrimid® irradiated with 450 keV H^+ ion represented by closed symbols or 3400 keV N^+ ions represented by open symbols.

CH_3 group. At increasing ion fluence, the degradation of the benzophenone C = O provided the partial reactive sites for the irradiation-induced crosslinking. For higher ion fluences (6×10^{14} H^+/cm^2 and beyond), both degradation of the para-disubstituted aromatic ring and rapid degradation of CH_3, benzophenone C=O, and the imide groups were observed. This degradation contributed to the high level of crosslinking of the irradiated Matrimid®.

While similar trends in degradation of backbone structure were observed for N^+ irradiation, the loss of functional groups was greater than for H^+ irradiation over much of the range of ion fluences used. Note that the ion fluences required to achieve similar total deposited energies were much lower for the N^+ irradiation. Irradiation at 5.9×10^{11} to 8.5×10^{11} N^+/cm^2 resulted in larger decay for the aliphatic stretch than the imide carbonyl and no change in aromatic ring stretch in this region. Since N^+ irradiation also resulted in partial crosslinking over this fluence range, degradation of both the aliphatic functional group and the imide C=O may contribute to the crosslinking. Since the benzophenone carbonyl C=O is more active and more sensitive to ion beam irradiation than the imide C=O, degradation of this group may also contribute to partial crosslinking (16).

As the N^+ fluence was increased from 4.2×10^{12} to 1.7×10^{13} N^+/cm^2, there was considerable degradation of the aliphatic group and the aromatic ring was increasingly susceptible to N^+ irradiation. Similar rapid degradation of structure were observed by Xu et.al. following the irradiation of polyimides with large ions (27). At higher ion fluences, the aromatic ring exhibited a sharp decay and the aliphatic stretch group had slowest degradation under N^+ irradiation. The reduced rate of degradation of the aliphatic stretch group may be due to residual formation of alphatic groups with degradation of other functional groups on polymer backbone. For example, degradation of the aromatic ring stretch due to the opening of the aromatic ring would involve the formation of new CH groups that would balance loss in functional groups from the backbone (28).

The general trend of the normalized areas of the three functional groups of the Matrimid® as a function of the total deposited energy for N^+ and H^+ irradiations are illustrated in Fig. 4(b). While ion fluence provides a convenient parameter to define irradiation conditions, the total deposited energy which accounts for the effect of ion mass and irradiation energy provides a better basis for comparison of the impact of irradiation on the polymer with different ion types. For the same total deposited energy, N^+ irradiation resulted in much larger degradation of the three functional groups than did H^+ irradiation. As the total

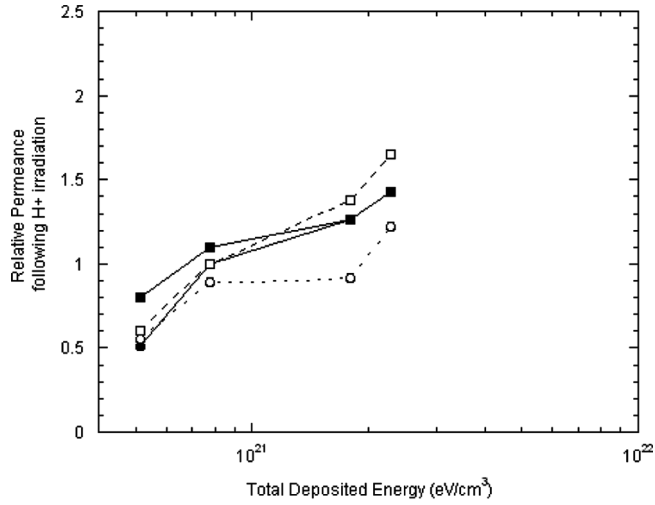

(a)

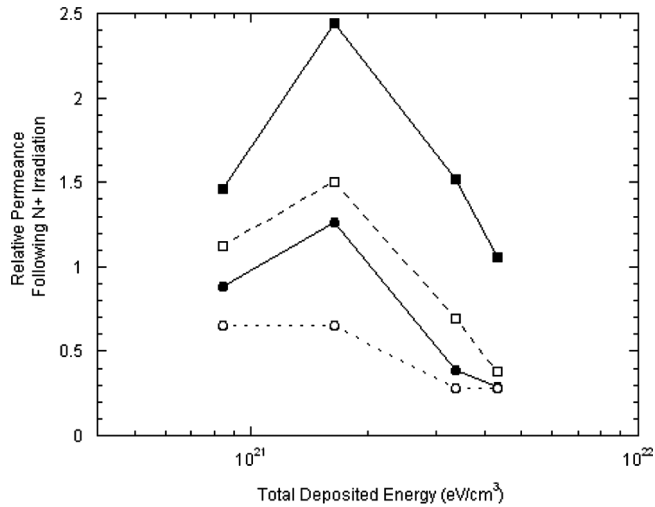

(b)

Figure 4. (a) Effect of the total deposited energy on the normalized permeances for He (■), CO_2 (●), O_2 (□) and CH_4 (○) in the Matrimid® -ceramic composite membranes irradiated by 180 keV H^+ ions (16). (b) Effect of the total deposited energy on the normalized permeances for He (■), CO_2 (●), O_2 (□) and CH_4 (○) in the Matrimid® -ceramic composite membranes irradiated by 400 keV N^+ ion.

deposited energy increased, the difference in the normalized area between N^+ and H^+ irradiation was larger. Over the entire range of total deposited energy used, the electronic energy loss for the H^+ and N^+ irradiation were very similar but N^+ exhibited greater percent nuclear energy loss. These results suggest that the nuclear energy loss contributed through collision between incident and target molecules contributed to the larger extent of degradation of Matrimid® resulted for N^+ irradiation despite a fairly small percentage of 2% in the total deposited energy. For irradiation at very low total deposited energy where the relative contribution nuclear energy loss is much smaller, the N^+ irradiated samples exhibited similar behavior to those observed for H^+ irradiation. These results are consistent with earlier studies that indicate that the ions with larger contribution from the nuclear loss mechanism will typically result in greater damage to polymer structure (29,30).

Evolution in Gas Permeation Properties

The large modification in chemical structure following N^+ irradiation is expected to result in significant evolution in the microstructure with corresponding modification of gas transport properties. Permeation of gas through a polymer membrane is a solution-diffusion process in which the gas molecules dissolve into the polymer on the high pressure side, diffuses across the polymer, and desorbs on the low pressure side (2). The permeability P_A is the product of a thermodynamic parameter S_A (i.e. the solubility coefficient) and a kinetic parameter D_A (i.e. the diffusion coefficient). The solubility coefficient is controlled by

(i) the overall fractional free volume and the distribution of the fractional free volume,
(ii) the inherent condensability of gas, and
(iii) interaction between polymer and gas (1).

Diffusive jumps of a penetrant within the polymer matrix occur when thermally activated motions of the polymer chain segments generate transient gaps between the polymer chains, which are larger than the sieving diameter of the penetrant. Chain packing, chain segmental mobility, and the size and shape of the penetrant determine the size and distribution of transient gaps required for diffusion to occur. Structural modifications of a polymer that inhibit chain packing or increase chain mobility to shift the distribution of transient gaps in the polymer matrix to larger sizes will increase the penetrant diffusivity (1). If these modifications also narrow, the distribution of transient gaps to retard the diffusion of one penetrant with respective to another, the diffusivity selectivity will increase.

Modification of formation of transient gaps required for diffusion can be achieved through synthesis of novel polymers or by postformation methods which change free volume or chain mobility. Simultaneously inhibiting intrasegmental motions and intrasegmental chain packing can increase both diffusivity and diffusivity selectivity (1).

Ion irradiation resulted in a loss of functional groups with some evolution of gas molecules following degradation of pendant groups that could result in the formation of small packing defects that would shift the free volume distribution to larger sizes. In addition, irradiation induced crosslinking would lead to a reduction in chain mobility effectively narrowing the distribution of free volume available for penetrant diffusion. Irradiation induced crosslinking will result in stiffening of the polymer matrix and degradation of functional groups could lead to formation of molecular scale defects that would increase free volume. The effect on the shape and peak location of the free volume distribution would depend upon the irradiation conditions (ion energy, fluence, and atomic mass) along with the extent of degradation of polymer.

The permeances and ideal permselectivities for five pure gases (He, CO_2, O_2, N_2, and CH_4) in the Matrimid®-ceramic composite before and after irradiation are listed in Tables 5 to 7. The normalized gas permeances of the Matrimid®-ceramic composite membranes induced by H^+ and N^+ irradiations as a function of total deposited energy are shown in Figs 4 (a) and (b). The normalized permeance, which is the ratio of the permeance of the Matrimid® composite membrane following irradiation to that of the virgin membrane, allows a direct comparison of the

Table 4. Pure gas permeances and permselectivities at 35°C in virgin Matrimid-ceramic composite membranes used for H^+ irradiation (16)

		Virgin membrane permeance (GPU)					Virgin membrane permselectivity		
Sample ID	Estimated thickness[a]	He	CO_2	O_2	N_2	CH_4	He/CH_4	O_2/N_2	CO_2/CH_4
H^+−1	0.3	77.0	38.0	7.28	1.37	1.33	29	5.3	29
H^+−2	0.5	59.7	19.5	4.66	0.90	0.79	25	5.2	25
H^+−3	1.2	27.2	10.8	1.94	0.38	0.38	29	5.2	29
H^+−4	1.3	21.8	9.9	1.75	0.30	0.27	37	5.9	37

[a]unit: μm based on the permeance of O_2 of the Matrimid®-ceramic composite membrane and the permeability of O_2 of the bulk material (3).

[b]1Barrer $= 10^{-10}$ cm^3 (STP) $cm/cm^3 \cdot s \cdot cmHg$; feed pressure: 55 psig.

[c]Ratio of pure-gas permeability.

Table 5. Permeation properties at 35°C of Matrimid®-ceramic composite membranes following 180 keV H^+ irradiation (16)

		H^+ Irradiated membrane permeance (GPU)					H^+ Irradiated membrane permselectivity		
Sample ID	Ion fluence (H^+/cm^2)	He	CO_2	O_2	N_2	CH_4	He/CH_4	O_2/N_2	CO_2/CH_4
H^+-1	6.0×10^{14}	61.4	19.4	4.4	0.82	0.73	84.1	5.4	26.6
H^+-2	9.0×10^{14}	65.2	19.5	4.7	0.93	0.70	93.1	5.1	27.9
H^+-3	2.0×10^{15}	37.0	13.6	2.7	0.48	0.35	105.7	5.6	38.9
H^+-4	2.5×10^{15}	36.9	14.2	2.9	0.45	0.33	111.8	6.4	43.0

[a]unit: μm based on the permeance of O_2 of the Matrimid®-ceramic composite membrane and the permeability of O_2 of the bulk material (3).
[b]1Barrer = 10^{-10} cm^3 (STP) $cm/cm^3 \cdot s \cdot cmHg$; feed pressure: 55 psig.
[c]Ratio of pure-gas permeability.

modification induced by ion beam irradiation at different conditions. Since the total deposited energy provides a better basis for comparison of the impact of ion irradiation on the structure and property evolution of polymers, the permeation results are presented in terms of total deposited energy along with relative contributions from nuclear and electronic energy loss. A detailed study of the evolution in gas permeation properties induced by H^+ irradiation was reported in an earlier paper, therefore,

Table 6. Pure gas permeances and permselectivities at 35°C in virgin Matrimid-ceramic composite membranes used for N^+ irradiation

		Virgin membrane permeance (GPU)					Virgin membrane selectivity		
Sample ID	Estimated Thickness[a]	He	CO_2	O_2	N_2	CH_4	He/CH_4	O_2/N_2	CO_2/CH_4
N^+-1	0.7	32	16.3	3.2	0.54	0.48	67	5.9	34
N^+-2	0.8	36	13.7	2.8	0.42	0.40	90	6.7	34
N^+-3	0.7	34	15.7	3.2	0.58	0.47	71	5.5	33
N^+-4	0.6	40	18.3	3.7	0.57	0.43	93	6.5	4.

[a]unit: μm based on the permeance of O_2 of the Matrimid®-ceramic composite membrane and the permeability of O_2 of the bulk material (3).
[b]1Barrer = 10^{-10} cm^3 (STP) $cm/cm^3 \cdot s \cdot cmHg$; feed pressure: 55 psig.
[c]Ratio of pure-gas permeability.

Table 7. Permeation properties at 35°C of Matrimid®-ceramic composite membranes following 400 keV N^+ irradiation

		N^+ Irradiated membrane permeance (GPU)					N^+ Irradiated membrane perms-electivity		
Sample ID	Ion fluence (N^+/cm^2)	He	CO_2	O_2	N_2	CH_4	He/CH_4	O_2/N_2	CO_2/CH_4
H^+–1	6.0×10^{14}	46	14.3	3.6	0.48	0.31	146	7.5	46.1
H^+–2	9.0×10^{14}	88	17.3	4.2	0.61	0.26	340	6.9	66.5
H^+–3	2.0×10^{15}	51	6.2	2.2	0.23	0.13	392	9.5	47.7
H^+–4	2.5×10^{15}	42	5.3	1.4	0.16	0.12	351	8.8	44.1

[a]unit: μm based on the permeance of O_2 of the Matrimid®-ceramic composite membrane and the permeability of O_2 of the bulk material (3).

this discussion will focus on impact of N^+ irradiation and a comparison of the effect of the irradiating ion on permeation properties (17). Note all samples used for permeation studies were irradiated in the range of total deposited energies that resulted in crosslinking for free standing films used for FTIR and dissolution studies.

The general trend in normalized permeances as a function of total deposited energy following H^+ irradiation is quite different from the trends observed for N^+ irradiation. As discussed in the previous section, H^+ irradiation resulted in some degradation of polymer structure at the irradiation conditions used for this study but the polymer maintained much of the original backbone structure. By contrast, N^+ irradiated samples had less than 20% of the original area of FTIR peaks so that the degradation of polymer structure was much greater. This difference in degradation would impact the microstructure of the polymer and the resulting gas transport properties.

In the case of H^+ irradiation, the normalized permeances for four smaller gases (He, CO_2, O_2, N_2) increased with total deposited energy with no distinguishable maximum. A similar trend was observed for CH_4 with the exception of a slight decrease in permeance following low energy irradiation. N^+ irradiation resulted in very different trends in relative permeance as a function of total deposited energy. Specifically, the normalized permeance exhibited a maximum at 1.64×10^{21} ev/cm^3 with a sharp decrease at higher total deposited energies. Therefore, as shown in Fig. 5, H^+ irradiation led to small increases in permselectivities.

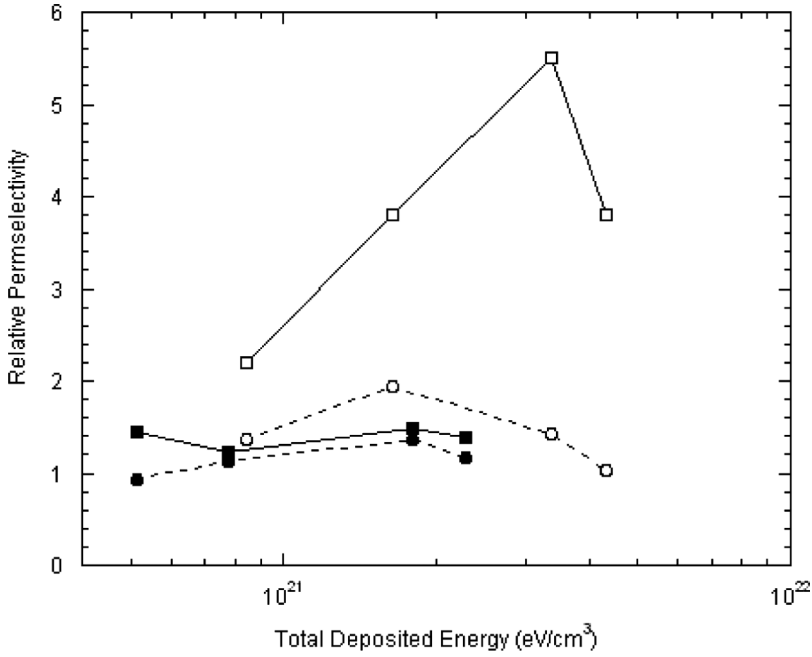

Figure 5. Impact of ion type and total deposited energy on the normalized permselectivities for the gas pairs CO_2/CH_4 (○,●), and He/CH_4 (□,■) of the Matrimid®-ceramic composite membranes where open symbols represent the 400 keV N^+ irradiated samples and closed symbols represent the 180 keV H^+ irradiated samples.

There was a large decrease in CH_4 permeability over the entire total deposited energy range.

N^+ irradiation at lower deposited energies resulted in similar changes in gas permeation properties of the Matrimid® to samples modified using H^+ irradiation. For example, there were 40% and 10% increases in He and O_2 permeabilities, respectively, with decreases in permeabilities for CO_2 by 12%, N_2 by 11%, and CH_4 by 34%. This resulted in increases in permselectivities for several gas pairs as shown in Fig. 5. At ion fluence of $2 \times 10^{14}\,N^+/cm^2$ corresponding to the total deposited energy loss of $8.45 \times 10^{20}\,eV/cm^3$, N^+ irradiation resulted in increases in both He and O_2 permeabilities, small decreases in CO_2 and N_2 permeabilities but large decrease in CH_4 permeability. Crosslinking would lead to increased stiffness of matrix combined with the evolution of small molecules following degradation of functional group. This could result in the generation of molecular scale packing defects which could be reflected in a slight

increase in free volume. The impact of N^+ irradiation on gas permeation is consistent with a slight increase fractional free volume and a shift of the free distribution to smaller size. Similar results were observed for H^+ irradiation at $9 \times 10^{14}\,H^+/cm^2$ or $7.85 \times 10^{20}\,eV/cm^3$.

There was a maximum increase in permeabilities for He, CO_2, O_2, and N_2 and a decrease in CH_4 permeability following irradiation at ion fluence of $4 \times 10^{14}\,N^+/cm^2$ corresponding to the total deposited energy of $1.6 \times 10^{21}\,eV/cm^3$. For example, there was a 2.4 fold in He permeability but significant reduction in the CH_4 permeability. This simultaneously contributed to large increases in permselectivities for several gas pairs (i.e. He/CH_4 by 265%, CO_2/CH_4 by 88%) and little change for O_2/N_2.

As the ion fluence and total deposited energy were further increased, only the He exhibited increases in permeability following N^+ irradiation. The large difference in the N^+ irradiation induced variation in gas permeabilities for five gases contributed to the very large increases in permselectivities. When ion fluence was $8 \times 10^{14}\,N^+/cm^2$ corresponding to at a total deposited energy of $3.4 \times 10^{21}\,eV/cm^3$, N^+ irradiation resulted in an increase in He permeability, a small decrease in O_2 permeability, and large decreases in the permeabilities for CO_2, N_2 and CH_4. This is quite different from what was observed for H^+ irradiation at $2.5 \times 10^{15}\,H^+/cm^2$ and $2.28 \times 10^{21}\,eV/cm^3$ (i.e. the permeabilities for all gases were slightly increased associated with improvement in permselectivities for most gas pairs).

Irradiation with N^+ at higher total deposited energy resulted in large decreases in all of the gas permeabilities relative to virgin membranes. In this range, there was significant degradation of pendant functional groups of polymer backbone that would provide steric hinderance to chain packing. This loss of groups could result in a collapse of polymer structure with a corresponding decrease in the fractional free volume. Therefore, N^+ irradiation at high ion fluence may result in a significant decrease of the fractional free volume. This is consistent with the significant decrease in permeability for all gases studied relative to virgin samples with no significant improvement in permselectivity following irradiation at high total deposited energy. As a result, ion beam irradiation at very high total deposited energy will not be advantageous to improve gas permeation properties of the polymer.

The permeation results indicated that the variation in microstructure induced by N^+ irradiation is different from that induced by H^+ irradiation. The differences in permeances following irradiation can be discussed in terms of the energy loss mechanisms for these two ions and the impact on chemical and microstructure evolution. For 400 keV N^+ and 180 keV H^+ ions used to irradiate the composite Matrimid® membranes, the percentage of the nuclear energy loss in the total deposited energy were cal-

culated using SRIM analysis at about $6 \sim 8\%$ and 0.1%, respectively. N^+ irradiation resulted in larger alteration in the gas permeabilities at smaller total deposited energy than H^+ irradiation. In addition, the shapes of the relative permeability versus deposited energy curves were different for the two irradiating ions. For example, N^+ irradiation at the total deposited energy of 1.6×10^{21} eV/cm^3, where the percentage of the nuclear energy loss was about 7%, exhibited a peak increase in permeability for each of the four small gases with large decrease of 33% in CH_4 permeability. However, H^+ irradiation a similar total deposited energy with a nuclear energy loss is only 0.1%, result in permeability increases of up to 40% for the smaller gases and an 8% decrease for CH_4. The large difference in modification in gas transport properties of the Matrimid®-ceramic composite membranes following N^+ and H^+ irradiations are consistent with literature report that the nuclear energy loss is critical in determining the property evolutione (33,39).

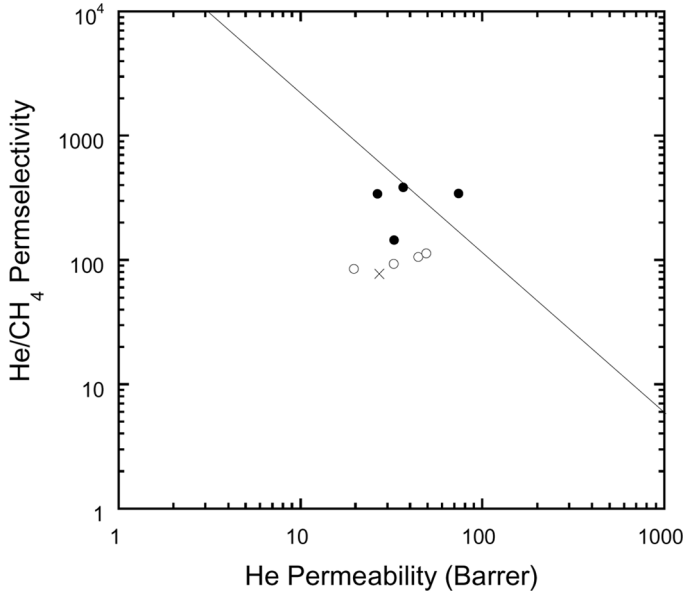

Figure 6. Tradeoff curve for He and He/CH_4 for virgin (X), H^+ membranes (○) and N^+ irradiated Matrimid®-composite membranes (●). The solid line represents the trade off curve for polymeric materials compiled by Robeson et. al. (2).

Trade-off Curves for He/CH_4 and CO_2/CH_4

Permeability-permselectivities trade off curves identified by Robeson et al. provide an useful means to compare the impact of irradiation conditions on the gas permeation properties of the Matrimid® (2). The permeabilities estimated using the product of measured permeance and an estimated thickness of the selective layer allow comparison of evolution of bulk polymer properties and eliminate differences due to membrane selective layer thickness. The selective layer thickness was estimated using the reported O_2 permeability of the bulk material and O_2 permeance of the virgin membrane (3). Specifically, the He/CH_4 and CO_2/CH_4 for the bulk and ion irradiated Matrimid® used in this study are plotted along with the trade-off curve for typical polymers is plotted in Figs. 6 and 7. In the case of the He/CH_4 gas pair, the bulk Matrimid® was well below the trade-off curve and there was a general shift toward the trade-off curve following ion irradiation. Though there was an increase in permeability following H^+ irradiation, there was little change in permselectivity. N^+ irradiation resulted in larger improvements

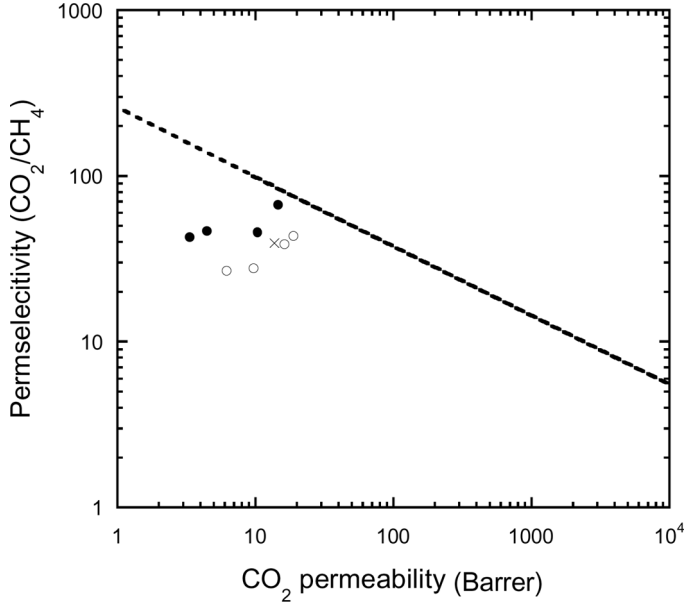

Figure 7. Tradeoff curve for CO_2 and CO_2/CH_4 for bulk Matrimid® (x), H^+ irradiated composite membranes (○) and N^+ irradiated membranes (●). The solid line represents the trade off curve for polymeric materials compiled by Robeson (2).

in the permeation properties relative to the bulk polymer with largest improvements occurring at intermediate fluences where the sample exhibited behaviors that were beyond the trade-off curve.

The modification of permeation properties for the CO_2/CH_4 gas pair relative to the bulk Matrimid® was complicated by the fact that CO_2 is very condensable and has a high solubility particularly in regions of excess free volume. Modifications to the polymer backbone which reduce this excess free volume including reduction in steric hinderance or irradiation induced relaxation could balance out any increases in diffusivity. This was reflected in the sharp decrease in CO_2 permeability with little change in permselectivity following N^+ irradiation at higher fluences. While ion beam irradiation provides an attractive means to simultaneously increase permeability and permselectivity of thin polymer selective layer without affecting the porous support, careful selection of irradiation conditions is necessary to optimize material properties.

CONCLUSION

This paper presented a comparison of the impact of H^+ and N^+ irradiation at similar total deposited energies on the backbone structure and permeation properties of the polyimide, Matrimid®. Ion irradiation resulted in a general evolution in structure of the polyimide with loss of pendant groups and degradation of the Matrimid® backbone. There was a trend of increase in permeance and permselectivity at lower fluences for the N^+ irradiated samples with a maximum in both the permeability and permselectivities at around $4 \times 10^{14}\ N^+/cm^2$. For example, irradiation at $4 \times 10^{14}\ N^+/cm^2$ resulted in a 2.5 fold increase in He permeability and 3.5 fold increase in He/CH_4 permselectivity. No such maximum in permeabilities occurred following H^+ irradiation over the range of fluences or total deposited energies studied. Irradiation with H^+ ions beyond the range used for this study was impractical because of the very long times required for irradiation at higher fluences (>2 hours).

N^+ irradiation resulted in larger change in chemical structure, microstructure, and gas permeation of Matrimid® than H^+ irradiation particularly at higher total deposited energy. Both the electronic energy and the nuclear energy loss mechanisms control the modification for N^+ irradiation but there was a larger contribution to modification from nuclear energy loss. The electronic energy loss was predominant for H^+ irradiation and the nuclear energy loss was negligible. These results are consistent with literature reports where ions of larger mass tend to result in greater damage from the nuclear energy loss relative to electronic energy loss to the target polymer. Ion beam irradiation can be used to simultaneously increase the

permeability and permselectivity within isolated thin selective layer of polymeric membranes. However, careful selection of ion type and irradiation conditions is necessary to optimize gas transport properties.

ACKNOWLEDGEMENT

The support of the National Science Foundation through the Presidential Faculty Fellows (CTS-955367) and CTS 9975452 in funding this project is acknowledged. In addition the authors would like to thank Dr. Peter Simpson of the University of Western Ontario for providing irradiation of the samples.

REFERENCES

1. Koros, W.J.; Coleman, M.R.; Walker, D.R.B. (1992) Controlled permeability polymer membranes. *Annu. Rev. Mater. Sci.*, *22*: 47–89.
2. Robeson, L.M. (1991) Correlation of separation factor versus permeability for polymeric membranes. *Journal of Membrane Science*, *62*: 165–185.
3. Bos, A. (1996) High pressure CO_2/CH_4 separation with glassy polymer membranes-Aspects of CO_2-induced plasticization, Ph.D. Dissertation, Membrane Technology Group, The University of Twene.
4. Rezac, M.E.; Sorensen, E.T.; Beckham, H.W. (1997) Transport properties of crosslinkable polyimide blends. *Journal of Membrane Science*, *136*: 249–259.
5. Staudt-Bickel, C.; Koros, W.J. (1999) Improvement of CO_2/CH_4 separation characteristic of polyimides by chemical crosslinking. *Journal of Membrane Science*, *155*: 145–154.
6. Liu, Y.; Wang, R.; Chung, T.S. (2001) Chemical cross-linking modification of polyimide membranes for gas separation. *Journal of Membrane Science*, *189*: 231–239.
7. Bos, A.; Punt, I.G.M.; Wessling, M.; Strathmann, H. (1998) Plasticization-resistant glassy polyimide membranes for CO_2/CH_4 separations. *Separation and Purification Technology*, *14*: 27–39.
8. Langsam, M. Fluorinated polymeric membranes for gas separation processes, US Pat 4,657,564 (1987).
9. Mohr, J.M.; Paul, D.R.; Pinnau, I.; Koros, W.J. (1991) Surface fluorination of polysulfone asymmetric membranes and films. *Journal of Membrane Science*, *56*: 77–98.
10. Roux, J.D.L.; Paul, D.R.; Kampa, J.; Lagow, R.J. (1994) Modification of asymmetric polysulfone membranes by mild surface fluorination: Part 1 Transport properties. *Journal of Membrane Science*, *94*: 121–141.

11. Kawakami, M.; Yamashita, Y.; Iwamoto, M.; Kagawa, S. (1984) Modification of gas permeabilities of polymer membranes by plasma coating. *Journal of Membrane Science*, *19*: 249–258.
12. Kramer, P.W.; Yeh, Y.S.; Yasuda, H. (1989) Low temperature plasma for the preparation of separation membranes. *Journal of Membrane Science*, *46*: 1–28.
13. Matsuyama, H.; Teramoto, M.; Hirai, K. (1995) Effect of plasma treatment on CO_2 permeability and selectivity of poly(dimethylsiloxane) membrane. *Journal of Membrane Science*, *99*: 139–147
14. Keil, M.; Rastomjee, C.S.; Rajagopal, A. (1998) Argon plasma-induced modifications at the surface of polycarbonate thin films. *Applied Surface Science*, *125*: 273–286.
15. Ruaan, R.C.; Wu, T.H.; Chen, S.H.; Lai, J.Y. (1998) Oxygen/Nitrogen separation by polybutadiene/polycarbonate composite membranes modified by ethylenediamine plasma. *Journal of Membrane Science*, *138*: 213–220.
16. Hu, L.; Xu, X.L.; Ilconich, J.R.; Ellis, S.; Coleman, M.R. (2003) Impact of H^+ ion irradiation on matrimid®. I. evolution in chemical structure. *Journal of Applied Polymer Science*, *90*: 2010.
17. Hu, L.; Xu, X.L.; Coleman, M.R. (2007) Impact of H^+ ion irradiation on matrimid (Π): Evolution in gas transport properties. *Journal of Applied Polymer Science*, *103*: 1670–1680.
18. Xu, X.L.; Dolveck, J.Y.; Boiteux, G.; Escoubes, M.; Monchanin, M.; Dupin, J.P.; Davenas, J. (1995) A new approach to microporous materials–application of ion beam technology to polyimides membranes. *Mat. Res. Soc. Symp. Proc.*, *354*: 351–356.
19. Xu, X.L.; Dolveck, J.Y.; Boiteux, G.; Escoubes, M.; Monchanin, M.; Dupin, J.P.; Davenas, J. (1995) Ion beam irradiation effect on gas permeation properties of polyimide films. *Journal of Applied Polymer Science*, *55*: 99–105.
20. Radjabov, T.D.; Alimova, L.Ya.; Djamaletdinova, I.E. (1989) Modification of gas-selective properties of polymer membranes by thin film deposition and carbon ion implantation. *Nuclear Instruments and Methods in Physics Research Section B*, *43*: 176–180.
21. Xu, X.L.; Coleman, M.R.; Myler, U.; Simpson, P.J. (2000) Postsynthesis Method for development of membranes using ion beam irradiation of polyimide thin films, Chapter 14 in American Chemical Society Symposium Series, 744. *Membrane Formation and Modification*, 205–227.
22. Escoubes, M.; Dolveck, J.Y.; Davenas, J.; Xu, X.L.; Boiyeux, G. (1995) Ion beam modification of polyimide membranes for gas permeation. *Nuclear Instruments and Methods in Physics Research Section B*, *105*: 130–133.
23. Xu, X.L.; Coleman, M.R. (1999) Preliminary investigation of gas transport mechanism in a H^+ irradiated polyimide-ceramic composite membrane. *Nucl. Instr. and Meths B*, *152*: 325–334.
24. Won, J.; Kim, M.H.; Kang, Y.S.; Park, H.C.; Kim, U.Y.; Choi, S.C.; Koh, S.K. (2000) Surface modification of polyimide and polysulfone membranes by ion beam for gas separation. *Journal of Applied Polymer Science*, *75*: 1554–1560.

25. Ilconich, J.R.; Xu, X.L.; Hu, L.; Coleman, M.R. (2003) Impact of ion beam irradiation on microstructure and gas permeance of polysulfone asymmetric membranes. *Journal of Membrane Science*, *214*: 143–156.
26. Nastasi, M.; Mayer, J.W.; Hirvonen, J.K. (1996) In: *Ion–Solid Interactions: Fundamentals and Applications*, Clarke, D.R.; Suresh, S.; Ward FRS, I.M., eds.; Cambrige University Press.
27. Xu, D.; Xu, X.L.; Du, G.D.; Wang, R.; Zou, S.C. (1993) Infrared analysis of the irradiation effects in aromatic polyimide films. *Nucl. Instr. and Meths. B*, *80–81*: 1063–1066.
28. Guenther, M.; Sahre, K.; Suchaneck, G.; Gerlach, G.; Eichhorn, K.J. (2001) Influence of ion-beam induced chemical and structural modification in polymers on moisture. *Surface and Coating Technology*, *142–144*: 482–288.
29. Davenas, J.; Xu, X.L.; Boiteux, G.; Sage, D. (1989) Relation between structure and electronic properties of ion irradiated polymers. *Nucl. Instr. and Meths. B*, *39*: 754–763.
30. Balanzat, E.; Betz, N.; Bouffard, S. (1995) Swift heavy ion modification of polymers. *Nucl. Instr. and Meths. B*, *105*: 46–54.
31. Koul, S.L.; Campbell, I.D.; Mcdonald, D.C. (1988) Energy transfer mechanisms and the radiation chemistry of noble gas ion irradiated polymers. *Nucl. Instr. and Meth. B*, *32*: 186–193.
32. Švorčík, V.; Rybka, V.; Stibor, I.; Hnatowicz, V.; Kvítek, J. (1995) Electrical conductivity of ion implanted polyimide. *Journal Electrochemical Society*, *142*: 590.
33. Švorčík, V.; Miček, I.; Rybka, V. (1997) Polyimide degradation induced by irradiation with N^+ ions. *Journal of Material Research*, *12*: 1661–1665.
34. Steckenreiter, T.; Balanzat, E.; Fuess, H.; Trautmann, C. (1999) Chemical degradation of polyimide and polysulfone films under the irradiation with heavy ions of several hundred meV. *J. Polym. Sci. Polym. Chem. Ed.*, *A37*: 4318–4329.
35. Švorčík, V.; Arenholz, E.; Rybka, V.; Hnatowicz, V. (1997) AFM surface morphology investigation of ion beam modified polyimide. *Nucl. Instr. and Meth. B*, *122*: 663–667.
36. Hnatowicz, V.; Peřina, V.; Havránek, V.; Voseček, V.; Novotný, J.; Vacík, J.; Švorčík, V.; Rybka, V.; Kluge, A. (2000) Degradation of polyimide and polyethyleneterephtalate irradiated with 150 and 200 keV Ar^+ ions, studied by RBS and ERD techniques. *Nucl. Instr. and Meth. B*, *161–163*: 1099–1103.
37. Guenther, M.; Sahre, K.; Suchaneck, G.; Gerlach, G.; Eichhorn, K.-J. (2001) Influence of ion-beam induced chemical and structural modification in polymers on moisture uptake. *Surface and Coating Technology*, *142–144*: 482–488.
38. Chung, T.-S.; Chan, S.; Wang, R.; Lu, Z.; He, C. (2003) Characterization of permeability and sorption in Matrimid/C60 mixed matrix membranes". *JMS*, *211*: 91–99.